

forbidden transitions (${}^4A_{2g} \rightarrow {}^2E_g$) of d^3 configuration in an effective octahedral field. A special feature of the Cr(III)-Mn(II) spectrum is a very sharp band at 420 nm ($\epsilon \sim 123 \text{ M}^{-1} \text{ cm}^{-1}$), which is assigned to the single excitation (${}^6A_1 \rightarrow {}^4E^4A_1$) at the Mn(II) center.

4. The oxidized species Cr(III)-M(III) ($M = \text{Mn, Fe, and Co}$) obtained by the electrochemical oxidation seems to be stable on the voltammetric time scale, and hence, the chemical preparation of the oxidation products should be feasible.

Acknowledgment. We thank the Fonds der Chemischen In-

dustrie for financial support of this work. Our thanks are also due to Prof. Dr. W. Haase and Dipl. Chem. S. Gehring (Darmstadt) for the low-temperature susceptibility measurements.

Supplementary Material Available: Listings of intraligand bond angles and distances, hydrogen atom coordinates, and anisotropic and isotropic thermal parameters for the Cr(III)-Fe(II) complex and anisotropic thermal parameters and hydrogen atom coordinates and isotropic thermal parameters for the Cr(III)-Co(II) complex (20 pages); listings of observed and calculated structure factors (76 pages). Ordering information is given on any current masthead page.

Contribution from the Department of Chemistry and Laboratory for Molecular Structure and Bonding, Texas A&M University, College Station, Texas 77843

Synthesis, Solid-State and Solution Structure, and Physicochemical Properties of the Iodide-Bridged Face-Sharing Bioctahedral Molybdenum(III) Dimers $[\text{Cat}]^+[\text{Mo}_2\text{I}_7(\text{PMe}_3)_2]^-$ (Cat = PHMe₃, NMe₄, AsPh₄)

F. Albert Cotton* and Rinaldo Poli

Received March 13, 1987

The compound $[\text{PHMe}_3][\text{Mo}_2\text{I}_7(\text{PMe}_3)_2]$ (**1**) has been obtained from $\text{Mo}_2\text{I}_4(\text{PMe}_3)_4$ and I_2 in toluene. The reaction of $\text{MoI}_3(\text{THF})_3$ with PMe_3 and NMe_4I in a 2:2:1 molar ratio affords $[\text{NMe}_4][\text{Mo}_2\text{I}_7(\text{PMe}_3)_2] \cdot 2\text{THF}$ (**2**) while $[\text{AsPh}_4][\text{Mo}_2\text{I}_7(\text{PMe}_3)_2]$ (**3**) has been obtained from **2** by metathesis with AsPh_4Cl . Crystal data: for compound **1**, monoclinic, space group $P2_1/n$, $a = 12.928$ (10) Å, $b = 23.206$ (12) Å, $c = 10.648$ (9) Å, $\beta = 110.95$ (6)°, $V = 2983$ (8) Å³, $Z = 4$, $R = 0.0623$ ($R_w = 0.0923$) for 180 parameters and 2202 unique data having $F_o^2 > 4\sigma(F_o^2)$; for compound **3**, orthorhombic, space group $P2_12_12_1$, $a = 14.347$ (3) Å, $b = 19.349$ (4) Å, $c = 8.076$ (1) Å, $V = 2242.0$ (7) Å³, $Z = 2$, $R = 0.0385$ ($R_w = 0.0579$) for 161 parameters and 1643 unique data having $F_o^2 > 3\sigma(F_o^2)$. The compounds have a face-sharing bioctahedral structure with three bridging iodine atoms and two additional terminal iodine atoms and one phosphine group per molybdenum atom. The phosphine ligands are in the syn configuration in the solid state. Dissolution causes an equilibration with the gauche isomer to the statistical 1:2 mixture, with $k_1 = (7.67 \pm 0.14) \times 10^{-4} \text{ s}^{-1}$ and $k_{-1} = (3.83 \pm 0.07) \times 10^{-4} \text{ s}^{-1}$ in acetone at 20 °C. The Mo-Mo distance of 3.022 Å for both compounds **1** and **3** indicates a significant metal-metal interaction. The compounds show a temperature-dependent paramagnetism. A variable-temperature ¹H NMR study is reported.

Introduction

We have recently studied the decarbonylation reaction of $\text{MoI}_2(\text{CO})_3(\text{PR}_3)_2$ materials.¹⁻⁴ This reaction led to the formation of dimers containing a quadruple metal-metal bond, $\text{Mo}_2\text{I}_4(\text{PR}_3)_4$ and/or to disproportionation with formation of molybdenum(0) carbonyl derivatives and mononuclear molybdenum(III) iodide-phosphine complexes. Since molybdenum(III) complexes containing iodide had not been thoroughly studied before and are in principle expected to exhibit interesting metal-metal interactions in polynuclear species,⁵ we have examined the possibility of obtaining these materials by more selective routes. In pursuit of this goal, we have been able to synthesize the potentially useful tetrahydrofuran adduct $\text{MoI}_3(\text{THF})_3$,⁶ with the intention of using it as a starting material for ligand substitution reactions. As an alternative strategy, we tried to add I_2 oxidatively to the quadruply bonded molybdenum(II) dimers $\text{Mo}_2\text{I}_4(\text{PR}_3)_4$. The formation of the edge-sharing bioctahedral $\text{Mo}_2\text{I}_6(\text{dppm})_2$ [$\text{dppm} = \text{bis}(\text{diphenylphosphino})\text{methane}$] has been recently achieved in this way.⁷ Our attempt to prepare a similar edge-sharing bioctahedral $\text{Mo}_2\text{I}_6(\text{PMe}_3)_4$ resulted instead in the formation of the face-sharing bioctahedral $[\text{Mo}_2\text{I}_7(\text{PMe}_3)_2]^-$ ion, as well as other, as yet, un-

characterized products. This chemistry and an alternative synthesis of the anion from $\text{MoI}_3(\text{THF})_3$ are reported here, together with structural studies in the solid state (by X-ray techniques) and in solution (by ¹H NMR).

Experimental Section

All operations were performed under an atmosphere of prepurified argon with standard Schlenk-tube techniques. Solvents were purified by conventional methods and distilled under dinitrogen prior to use. Instruments used were as follows: IR, Perkin-Elmer 783; UV/visible, Cary-17; NMR, Varian XL-200. Elemental analyses were by Galbraith Laboratories Inc., Knoxville, TN. Magnetic susceptibility measurements were performed by the Gouy method as modified by D. F. Evans on a JME magnetic balance (Johnson Matthey). The compounds $\text{Mo}_2\text{I}_4(\text{PMe}_3)_4$ ¹ and $\text{MoI}_3(\text{THF})_3$ ⁶ were prepared according to published procedures.

Reaction between $\text{Mo}_2\text{I}_4(\text{PMe}_3)_4$ and I_2 in Toluene. Preparation of $[\text{PHMe}_3][\text{Mo}_2\text{I}_7(\text{PMe}_3)_2]$ (1**).** A 95-mg sample of the molybdenum(II) dimer (0.095 mmol) was treated in toluene (10 mL) with I_2 (24 mg, 0.095 mmol). Stirring at room temperature for a few hours caused no change. The solution was then warmed to the reflux temperature. A brown precipitate formed. This was filtered off and extracted with CH_2Cl_2 (3 mL), and the filtered solution was carefully layered with 5 mL of toluene. The red X-ray quality crystals that formed (compound **1**, 15 mg), were decanted, washed with hexane, and dried in vacuo. Anal. Calcd for $\text{C}_9\text{H}_{23}\text{I}_7\text{Mo}_2\text{P}_3$: C, 8.25; H, 2.15. Found: C, 8.41; H, 2.23. IR (Nujol mull): 1410 m, 1300 m, 1280 m, 1265 m, 960 s, 790 m, 735 m cm^{-1} .

Reaction of $\text{MoI}_3(\text{THF})_3$ with PMe_3 and NMe_4I in a 2:2:1 Molar Ratio. Preparation of $[\text{NMe}_4][\text{Mo}_2\text{I}_7(\text{PMe}_3)_2] \cdot 2\text{THF}$ (2**).** $\text{MoI}_3(\text{THF})_3$ (1.735 g, 2.50 mmol) was suspended in 20 mL of THF and treated with 0.25 mL of PMe_3 (2.5 mmol) and 0.287 g of NMe_4I (1.23 mmol). The mixture was stirred at room temperature for about 2 h and then refluxed overnight. The color of the solution had changed from red to yellow-

- (1) Cotton, F. A.; Poli, R. *J. Am. Chem. Soc.* **1986**, *108*, 5628.
- (2) Cotton, F. A.; Poli, R. *Inorg. Chem.* **1986**, *25*, 3624.
- (3) Cotton, F. A.; Dunbar, K. R.; Poli, R. *Inorg. Chem.* **1986**, *25*, 3700.
- (4) Cotton, F. A.; Poli, R. *Inorg. Chem.* **1986**, *25*, 3703.
- (5) (a) Cotton, F. A.; Wilkinson, G. *Advanced Inorganic Chemistry*, 4th ed.; Wiley: New York, 1980; p 864. (b) Cotton, F. A.; Ucko, D. A. *Inorg. Chim. Acta* **1972**, *6*, 161.
- (6) Cotton, F. A.; Poli, R. *Inorg. Chem.* **1987**, *26*, 1514.
- (7) Cotton, F. A.; Dunbar, K. R., manuscript in preparation.

Table I. Crystal Data for [Cat][Mo₂I₇(PMe₃)₂] (Cat = PHMe₃ (1), AsPh₄ (3))

	1	3
formula	C ₉ H ₂₈ I ₇ Mo ₂ P ₃	C ₃₀ H ₃₈ AsMo ₂ I ₇ P ₂
fw	1309.453	1615.72
space group	P2 ₁ /n	P2 ₁ 2 ₁ 2
syst abs	h0l, h + l ≠ 2n; 0k0, k ≠ 2n	h00, h ≠ 2n; 0k0, k ≠ 2n
a, Å	12.928 (10)	14.347 (3)
b, Å	23.206 (12)	19.349 (4)
c, Å	10.648 (9)	8.076 (1)
α, deg	90	90
β, deg	110.95 (6)	90
γ, deg	90	90
V, Å ³	2983 (8)	2242.0 (7)
Z	4	2
d _{calcd} , g/cm ³	2.915	2.393
cryst size, mm	0.1 × 0.2 × 0.8	0.15 × 0.20 × 0.7
μ(Mo Kα), cm ⁻¹	81.494	61.338
data collcn instrum	Syntex P3	Rigaku AFC5R
radiation (monochromated in incident beam)	Mo Kα (λ _K = 0.71073 Å)	Mo Kα (λ _K = 0.71073 Å)
orientation reflns: no.;	25; 20-25	25; 18-25
range (2θ), deg		
temp, °C	20	20
scan method	ω	ω-2θ
data collcn range (2θ), deg	4-45	4-50
no. of unique data, total obsd	3457, 2617 ^a	2306, 1643 ^b
no. of params refined	180	161
transmissn factors: max, min	0.999, 0.618	1.000, 0.369
R ^c	0.0666	0.0385
R _w ^d	0.0982	0.0579
quality-of-fit indicator ^e	1.939	1.260
largest shift/esd, final cycle	0.12	0.27
largest peak, e/Å ³	1.458	0.762

^a $F_o^2 > 4\sigma(F_o^2)$. ^b $F_o^2 > 3\sigma(F_o^2)$. ^c $R = \sum ||F_o| - |F_c|| / \sum |F_o|$. ^d $R_w = [\sum w(|F_o| - |F_c|)^2 / \sum w|F_o|^2]^{1/2}$; $w = 1/\sigma^2(|F_o|)$. ^e Quality of fit = $[\sum w(|F_o| - |F_c|)^2 / (N_{\text{observns}} - N_{\text{params}})]^{1/2}$.

brown during the thermal treatment, while the white insoluble NMe₄I had been replaced by black microcrystals of the product. After the mixture was cooled to room temperature, the solid was filtered off, washed with small portions of THF, and dried in vacuo. Yield: 1.153 g (63.5%). Anal. Calcd for C₁₈H₄₆I₇Mo₂NO₂P₂: C, 14.90; H, 3.20; N, 0.97. Found: C, 14.50; H, 3.10; N, 0.92. IR (Nujol mull): 1415 m, 1300 w, 1280 m, 1065 m, 955 s, 740 m cm⁻¹. ¹H NMR (CD₃COCD₃, 20 °C): 3.62 (m, br, THF, 8 H), 3.43 (s, NMe₄⁺, 12 H), 1.78 (m, br, THF, 8 H), -2.43 (s) and -3.12 (s) (PMe₃, 18 H). χ_M(20 °C) = 846 × 10⁻⁶. μ_{eff} = 1.83 μ_B (diamagnetic correction = -563 × 10⁻⁶).

Preparation of [AsPh₄][Mo₂I₇(PMe₃)₂] (3). Compound 2 (0.155 g, 0.107 mmol) was dissolved in 5 mL of acetone and treated with a solution of AsPh₄Cl (ca. 300 mg, excess) in 5 mL of methanol. X-ray quality crystals of the product formed promptly. After ca. 1/2 h the solvent was decanted, and the crystals were washed with MeOH and dried. Yield: 101 mg (58%). When the product was left to stand in the reaction mixture for a longer time, it slowly redissolved, presumably because of a reaction with the solvent, to afford uncharacterized products. Anal. Calcd for C₃₀H₃₈AsI₇Mo₂P₂: C, 22.30; H, 2.37. Found: C, 22.44; H, 2.41. IR (Nujol mull): 1435 s, 1415 w, 1410 w, 1300 w, 1285 w, 1280 w, 1085 w, 1080 w, 1000 w, 955 s, 950 sh, 745 m, 695 w, 680 w, 480 w, 460 w cm⁻¹. ¹H NMR (CD₂Cl₂, 20 °C): 8.0-7.7 (m, Ph, 20 H), -2.18 (s) and -2.84 (s) (PMe₃, 18 H).

X-ray Crystallography. Compound 1. A single crystal was put on the tip of a glass fiber and mounted on the diffractometer. Data collection and reduction were routine. Three standard reflections, which were monitored periodically during data collection, showed no significant variation of intensity. An absorption correction based on azimuthal (ψ) scans was applied according to the method of North, Phillips, and Mathews.⁸ The heavy atoms (Mo and I) were located by SHELXS-86 direct methods,⁹ and the rest of the structure was found by alternating least-squares full-matrix cycles of refinement and difference Fourier maps for a cutoff ratio $F_o^2/\sigma(F_o^2)$ of 3. The Enraf-Nonius SDP software was employed. All the atoms were then refined anisotropically. Atoms C(2)

Table II. Positional Parameters and Their Estimated Standard Deviations for [PHMe₃][Mo₂I₇(PMe₃)₂]

atom	x	y	z	B, Å ²
Mo(1)	0.1963 (2)	0.62065 (8)	0.3410 (2)	3.56 (5)
Mo(2)	0.3936 (2)	0.63346 (8)	0.2543 (2)	3.39 (5)
I(1)	0.0049 (2)	0.68690 (9)	0.2540 (2)	5.25 (5)
I(2)	0.0835 (2)	0.51876 (8)	0.3297 (3)	6.71 (6)
I(3)	0.3157 (2)	0.72175 (7)	0.3721 (2)	4.90 (5)
I(4)	0.3921 (2)	0.56184 (8)	0.4615 (2)	5.44 (5)
I(5)	0.1829 (2)	0.60369 (8)	0.0737 (2)	4.51 (4)
I(6)	0.4877 (2)	0.54511 (8)	0.1587 (2)	5.27 (5)
I(7)	0.4203 (2)	0.70774 (8)	0.0657 (2)	5.29 (5)
P(1)	0.1856 (7)	0.6307 (4)	0.5759 (7)	5.0 (2)
P(2)	0.5889 (7)	0.6662 (4)	0.3930 (8)	5.1 (2)
P(3)	0.2452 (9)	0.9208 (5)	0.432 (1)	8.3 (3)
C(1)	0.055 (3)	0.623 (1)	0.589 (3)	8 (1)
C(2)	0.230 (3)	0.699 (1)	0.650 (3)	6.6 (8)*
C(3)	0.264 (4)	0.575 (2)	0.701 (4)	13 (1)
C(4)	0.598 (3)	0.741 (1)	0.432 (4)	11 (1)
C(5)	0.694 (3)	0.659 (1)	0.320 (5)	9 (1)
C(6)	0.652 (4)	0.629 (2)	0.559 (5)	11 (1)*
C(7)	0.278 (3)	0.955 (2)	0.592 (4)	7 (1)
C(8)	0.142 (4)	0.869 (2)	0.417 (5)	11 (1)
C(9)	0.355 (3)	0.894 (1)	0.401 (5)	8 (1)

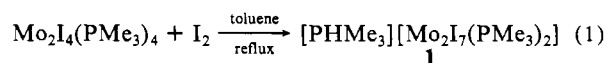
* Values marked with an asterisk denote isotropically refined atoms. Values for anisotropically refined atoms are given in the form of the equivalent isotropic displacement parameter defined as $\frac{1}{3}[a^2\beta_{11} + b^2\beta_{22} + c^2\beta_{33} + ab(\cos \gamma)\beta_{12} + ac(\cos \beta)\beta_{13} + bc(\cos \alpha)\beta_{23}]$

and C(6) were not well-behaved and were therefore left isotropic. Refinement converged at $R = 0.074$. An analysis of the calculated and observed structure factors showed higher deviations for the data with a low $F_o^2/\sigma(F_o^2)$ ratio. Refinement was continued with the data having $F_o^2/\sigma(F_o^2) > 4$, and convergence was achieved at $R = 0.0666$. Hydrogen atoms were not located. Crystal data are reported in Table I. Table II shows the fractional atomic coordinates, while selected bond distances and angles are listed in Table III.

Compound 3. A parallelepiped-shaped crystal was glued on the tip of a glass fiber and mounted on a computer-controlled diffractometer equipped with a rotating-anode X-ray source. Preliminary operations and collection of intensity data were routine. Pertinent data are given in Table I. Three standard reflections, which were periodically monitored during data collection, showed no significant variation of intensity. The data were corrected for Lorentz and polarization effects, and a semi-empirical absorption correction was also applied.⁸ Systematic absences from the data uniquely determined the space group as the orthorhombic P2₁2₁2. The heavy-atom part of the structure was found with direct methods by using the SHELXS-86 package.⁹ Subsequent alternate least-squares full-matrix cycles and difference Fourier maps revealed the rest of the structure. At the end of the isotropic refinement an additional absorption correction was applied.¹⁰ The structure was then refined anisotropically. Carbon atoms refined with non-positive-definite thermal tensors. They were therefore left isotropic. Final refinement was performed for both enantiomeric forms, and the one refining to the lowest R factor is reported. Fractional atomic coordinates are listed in Table IV and selected bond distances and angles are reported in Table III.

Results and Discussion

(a) Synthesis. While the oxidative addition of I₂ to Mo₂I₄(μ-dppm)₂ to afford Mo₂(μ-I)₂I₄(μ-dppm)₂ is fast at room temperature,⁷ we find that Mo₂I₄(PMe₃)₄ and I₂ do not react under the same conditions. When the solution is warmed to the reflux temperature of the solvent (toluene) a reaction takes place with formation of a precipitate. This is the salt [PHMe₃][Mo₂I₇(PMe₃)₂] (1) as shown by analytical data and by X-ray crystallography. The P-H stretching vibration (typically found for trialkylphosphonium cations (or triarylphosphonium) as a weak absorption at 2350 cm⁻¹)^{2,11} was not evident in the infrared spectrum.



(8) North, A. C. T.; Phillips, D. C.; Mathews, F. S. *Acta Crystallogr., Sect. A: Cryst. Phys., Diff., Theor. Gen. Crystallogr.* **1968**, *24*, 351.
(9) Sheldrick, G. M. "SHELXS-86", Institut für Anorganische Chemie der Universität, Göttingen, FRG, 1986.

(10) Walker, N.; Stuart, D. *Acta Crystallogr., Sect. A: Found. Crystallogr.* **1983**, *39*, 158.
(11) (a) Lewis, J.; Whyman, R. *J. Chem. Soc. A* **1967**, *77*. (b) Colton, R.; Rix, C. *J. Aust. J. Chem.* **1969**, *22*, 305.

Table III. Selected Bond Distances (Å) and Angles (deg) for the $[\text{Mo}_2\text{I}_7(\text{PMe}_3)_2]^-$ Anion in Compounds **1** and **3**

		1		3	
Mo-Mo	Mo(1)-Mo(2)	3.021 (4)	Mo-Mo'	3.022 (1)	
Mo-(μ-I)	Mo(1)-I(3)	2.762 (3)	Mo-I(2)	2.760 (4)	
	Mo(1)-I(4)	2.755 (3)	Mo-I(2)'	2.781 (4)	
	Mo(2)-I(3)	2.772 (3)			
	Mo(2)-I(4)	2.768 (3)			
	Mo(1)-I(5)	2.817 (3)	Mo-I(1)	2.790 (1)	
	Mo(2)-I(5)	2.801 (3)			
Mo-I	Mo(1)-I(1)	2.776 (2)	Mo-I(3)	2.744 (3)	
	Mo(1)-I(2)	2.758 (3)	Mo-I(4)	2.788 (3)	
	Mo(2)-I(6)	2.758 (3)			
	Mo(2)-I(7)	2.760 (3)			
Mo-P	Mo(1)-P(1)	2.565 (9)	Mo-P	2.546 (3)	
	Mo(2)-P(2)	2.543 (8)			
Mo-(μ-I)-Mo	Mo(1)-I(3)-Mo(2)	66.16 (8)	Mo-I(2)-Mo'	66.09 (6)	
	Mo(1)-I(4)-Mo(2)	66.32 (8)			
	Mo(1)-I(5)-Mo(2)	65.07 (8)	Mo-I(1)-Mo'	65.57 (3)	
(μ-I)-Mo-(μ-I)	I(3)-Mo(1)-I(4)	89.08 (4)	I(2)-Mo-I(2)'	88.43 (6)	
	I(3)-Mo(2)-I(4)	88.6 (1)			
	I(3)-Mo(1)-I(5)	94.0 (1)	I(1)-Mo-I(2)	95.73 (8)	
	I(4)-Mo(1)-I(5)	96.6 (1)	I(1)-Mo-I(2)'	95.26 (8)	
	I(3)-Mo(2)-I(5)	94.12 (9)			
	I(4)-Mo(2)-I(5)	96.72 (9)			
I-Mo-(μ-I)	I(1)-Mo(1)-I(3)	87.88 (8)	I(3)-Mo-I(2)	88.7 (1)	
	I(2)-Mo(1)-I(4)	88.80 (8)	I(4)-Mo-I(2)'	88.5 (1)	
	I(6)-Mo(2)-I(4)	88.71 (9)			
	I(7)-Mo(2)-I(3)	91.59 (9)			
	I(1)-Mo(1)-I(5)	90.84 (8)	I(3)-Mo-I(1)	90.36 (7)	
	I(2)-Mo(1)-I(5)	89.76 (9)	I(4)-Mo-I(1)	90.46 (7)	
	I(6)-Mo(2)-I(5)	90.71 (8)			
	I(7)-Mo(2)-I(5)	89.93 (8)			
	I(1)-Mo(1)-I(4)	172.1 (1)	I(3)-Mo-I(2)'	173.94 (7)	
	I(2)-Mo(1)-I(3)	175.9 (1)	I(4)-Mo-I(2)	173.31 (7)	
	I(6)-Mo(2)-I(3)	174.73 (9)			
	I(7)-Mo(2)-I(4)	173.3 (1)			
I-Mo-I	I(1)-Mo(1)-I(2)	93.76 (9)	I(3)-Mo-I(4)	93.76 (4)	
	I(6)-Mo(2)-I(7)	90.5 (1)			
P-Mo-(μ-I)	P(1)-Mo(1)-I(5)	173.2 (2)	P-Mo-I(1)	171.3 (1)	
	P(2)-Mo(2)-I(5)	172.8 (2)			
	P(1)-Mo(1)-I(3)	91.6 (2)	P-Mo-I(2)	92.5 (1)	
	P(1)-Mo(1)-I(4)	87.3 (2)	P-Mo-I(2)'	87.9 (1)	
	P(2)-Mo(2)-I(3)	87.8 (2)			
	P(2)-Mo(2)-I(4)	90.3 (2)			
P-Mo-I	P(1)-Mo(1)-I(1)	85.6 (2)	P-Mo-I(3)	86.9 (1)	
	P(1)-Mo(1)-I(2)	84.7 (2)	P-M-I(4)	81.5 (1)	
	P(2)-Mo(2)-I(6)	87.7 (2)			
	P(2)-Mo(2)-I(7)	83.1 (2)			

Table IV. Atomic Positional Parameters and Equivalent Isotropic Displacement Parameters and Their Estimated Standard Deviations for $[\text{AsPh}_4][\text{Mo}_2\text{I}_7(\text{PMe}_3)_2]$

atom	x	y	z	$B^a, \text{Å}^2$
Mo	0.0006 (3)	0.57809 (5)	0.7506 (1)	2.18 (2)
I(1)	0.000	0.500	0.4601 (1)	3.07 (2)
I(2)	0.13467 (7)	0.5005 (2)	0.9101 (1)	4.00 (2)
I(3)	0.13994 (8)	0.66004 (6)	0.6258 (1)	3.58 (2)
I(4)	-0.14149 (7)	0.66152 (6)	0.6260 (1)	3.50 (2)
P	-0.0102 (4)	0.6638 (2)	0.9891 (4)	2.96 (7)
C(1)	-0.014 (1)	0.7549 (8)	0.932 (2)	3.6 (3)*
C(2)	0.084 (1)	0.650 (1)	1.151 (2)	3.9 (4)*
C(3)	-0.113 (2)	0.664 (1)	1.117 (2)	4.7 (4)*
As	0.500	0.500	0.9480 (2)	2.48 (3)
C(10)	0.505 (2)	0.5797 (6)	0.806 (1)	2.9 (2)*
C(11)	0.587 (1)	0.389 (1)	0.763 (2)	3.5 (3)*
C(12)	0.587 (1)	0.3380 (8)	0.647 (2)	2.6 (3)*
C(13)	0.492 (2)	0.3138 (7)	0.582 (1)	3.2 (2)*
C(14)	0.421 (2)	0.348 (1)	0.628 (2)	5.2 (5)*
C(15)	0.582 (1)	0.5995 (8)	0.745 (2)	2.2 (2)*
C(20)	0.396 (1)	0.505 (2)	1.095 (1)	3.1 (2)*
C(21)	0.369 (1)	0.426 (1)	1.153 (2)	4.1 (4)*
C(22)	0.304 (1)	0.4266 (8)	1.281 (2)	3.0 (3)*
C(23)	0.272 (1)	0.487 (1)	1.352 (2)	4.0 (3)*
C(24)	0.300 (2)	0.551 (1)	1.302 (3)	5.1 (4)*
C(25)	0.363 (1)	0.5555 (9)	1.163 (2)	3.2 (3)*

^aSee footnote a in Table II.

We do not have any evidence concerning the origin of the phosphonium proton, but we observe that phosphonium cations are often formed when molybdenum-phosphine complexes are reacted in organic solvents. For example, I_2 oxidation of $\text{Mo}(\text{CO})_3(\text{PPh}_3)_3$ (solvent = CH_2Cl_2) afforded $[\text{PPh}_3][\text{MoI}_3(\text{CO})_3(\text{PPh}_3)]$ instead of the expected $\text{MoI}_2(\text{CO})_3(\text{PPh}_3)_2$.^{11a} The same compound was later obtained from $\text{Mo}_2\text{I}_4(\text{CO})_8$ and PPh_3 operating in the same solvent.^{11b} Baker and Fraser have recently been able to isolate $\text{MoI}_2(\text{CO})_3(\text{PPh}_3)_2$ from $\text{MoI}_2(\text{CO})_3(\text{MeCN})_2$ and PPh_3 and to observe its slow conversion into the phosphonium salt in dichloromethane.¹² This reactivity has apparently never been observed for the corresponding chloride and bromide compounds.

We recently reported that $\text{MoI}_2(\text{CO})_3(\text{PEt}_2\text{Ph})_2$, obtained in situ from $\text{Mo}_2\text{I}_4(\text{CO})_8$ and PEt_2Ph , disproportionates in THF to Mo(0) carbonyl derivatives and $[\text{PHEt}_2\text{Ph}][\text{MoI}_4(\text{PEt}_2\text{Ph})_2]$.² Interaction of MoI_3 and PEt_3 in a 1:3 molar ratio (solvent = toluene) leads to the analogous salt $[\text{PHEt}_3][\text{MoI}_4(\text{PEt}_3)_2]$ instead of the expected $\text{MoI}_3(\text{PEt}_3)_3$.⁶ The latter compound was then prepared from $\text{MoI}_3(\text{THF})_3$, and it could be converted thermally into the phosphonium salt in refluxing toluene.⁶ We now find that another phosphonium salt is obtained by oxidizing $\text{Mo}_2\text{I}_4(\text{PMe}_3)_4$ with I_2 . Our solvent is again toluene.

(12) Baker, P. K.; Fraser, S. G. *Inorg. Chim. Acta* **1986**, *116*, L1.

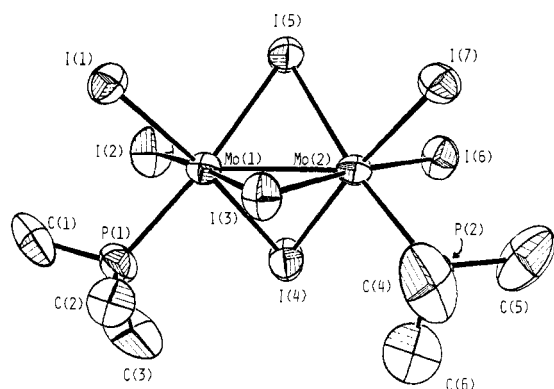
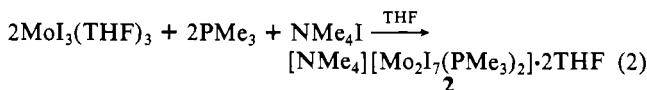


Figure 1. View of the $[\text{Mo}_2\text{I}_7(\text{PMe}_3)_2]^-$ anion in compound **1** with the atomic numbering scheme employed. The anion of compound **3** has an identical geometry with an atomic numbering scheme that correlates to the present one as follows (**1** \rightarrow **3**): Mo(1) \rightarrow Mo; I(5) \rightarrow I(1); I(3) \rightarrow I(2); I(4) \rightarrow I(2)'; I(1) \rightarrow I(3); I(2) \rightarrow I(4); P(1) \rightarrow P.

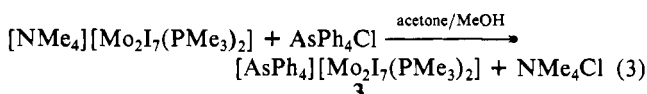
Although the intimate mechanism of these reactions has never been understood and is presumably very complicated, it seems probable that the proton source is the solvent (and not, for example, the phosphine). In fact, all the solvents employed for these reactions (i.e. CH_2Cl_2 , THF, toluene) contain somewhat labile C-H bonds. We repeated our reaction between $\text{Mo}_2\text{I}_4(\text{PMe}_3)_4$ and I_2 in benzene and we failed to isolate any amount of compound **1**.

The $[\text{Mo}_2\text{I}_7(\text{PMe}_3)_2]^-$ anion is also formed as its NMe_4^+ salt containing interstitial THF, compound **2**, in good yields by reacting the tetrahydrofuranate, $\text{MoI}_3(\text{THF})_3$,⁶ with the required amount of PMe_3 and NMe_4I according to the stoichiometry of eq 2.



Treatment of $\text{MoI}_3(\text{THF})_3$ with an excess of PMe_3 (and in the absence of NMe_4I) leads to the formation of $\text{MoI}_3(\text{PMe}_3)_3$ instead.⁶

Compound **2** is converted to the AsPh_4^+ salt, compound **3**, by metathesis, as shown in eq 3.



The solid-state infrared spectra of compounds **1**–**3** were, with the exception of bands attributable to the cation, essentially identical.

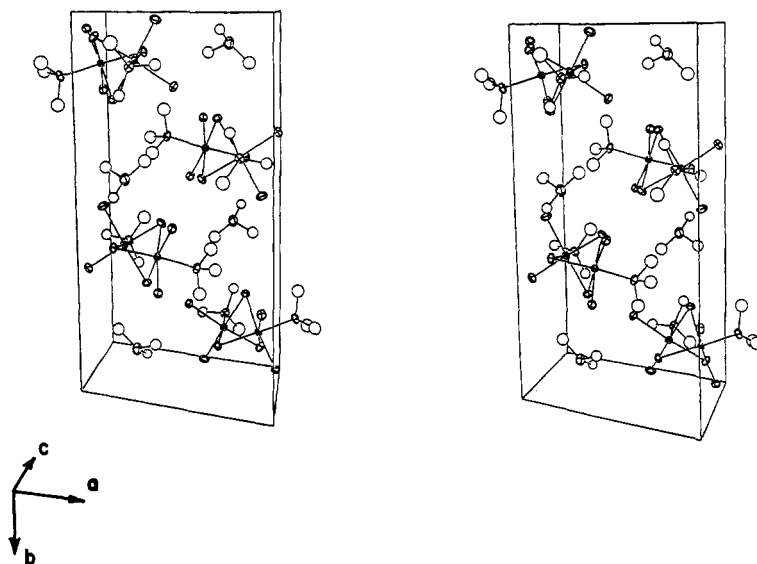


Figure 2. Stereoscopic view of the unit cell of compound **1**.

(b) Crystallographic Studies. Compound **1** crystallizes in the monoclinic space group $P2_1/n$, and no crystallographic symmetry is imposed on the molecule. The geometry of the anion, shown in Figure 1, is that of a face-sharing biocuboctahedron, with the three bridging iodine atoms determining the triangular shared face. Each molybdenum atom completes its coordination sphere with two terminal iodine atoms and a trimethylphosphine group. The two PMe_3 ligands are trans to the same bridging iodide, resulting in a syn configuration for the anion.

The hydrogen atom on the phosphonium cation was not located. The alternative assignment of a neutral mixed-valence Mo_2^{7+} species containing an interstitial PMe_3 molecule is then possible in principle. However, we reject this possibility in view of the identical structural parameters of **1** and the AsPh_4^+ salt, **3** (vide infra).

We were intrigued by the calculated volume per non-hydrogen atom of 35.5 \AA^3 , which is to be regarded as unusually high. Typical values are in the range $17\text{--}25 \text{ \AA}^3$. Such a high value for compound **1** could be at least partially due to the presence of several iodine atoms with a large van der Waals radius. In our opinion, however, this value is too high and there must be some other factor coming into play. A possible one is found by looking at the packing diagram shown in Figure 2. Four anions are packed in the unit cell so as to occupy about half of the volume and arranged pseudooctahedrally around the pockets where the cations sit. The small PHMe_3^+ cations sit right in the center of these relatively large pockets, leaving no possibility for the rest of the volume to be filled in with interstitial solvent molecules. In order to give support to this idea, we determined the crystal structure of compound **3**, which contains the larger AsPh_4^+ cation.

Compound **3** crystallizes in the noncentrosymmetric orthorhombic $P2_12_12$ space group. The geometry of the anion is the same as in compound **1**, including the syn configuration of the PMe_3 ligands. In the present case the anion sits on a crystallographic twofold axis that passes through the bridging I(1) atom and the middle of the Mo-Mo' bond.

Although the space group is different, the packing diagram of compound **3**, see Figure 3, is fairly similar to that of **1**, i.e. pseudocubic, the difference being that this time the cation is able to more fully occupy the volume left after packing of the anions. The result is, as anticipated, a smaller calculated volume per nonhydrogen atom, i.e. 26.7 \AA^3 . This too, is on the high side of the expected range, but we believe that this can be attributed to the large number of bulky iodine atoms.

Table III shows that all the structural parameters of the two anions compare well. In particular, the metal-metal distance is the same within experimental error. Such a distance is longer than those found for other face-sharing biocuboctahedral Mo_2^{6+} structures, e.g. $2.655(11) \text{ \AA}$ in $\text{Mo}_2\text{Cl}_9^{3-}$ and $2.816(9) \text{ \AA}$ in

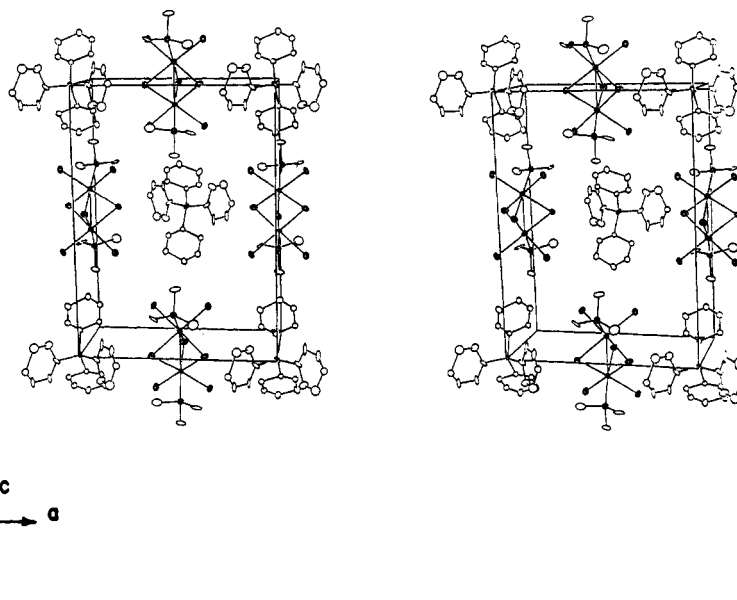


Figure 3. Stereoscopic view of the unit cell of compound 3.

$\text{Mo}_2\text{Br}_9^{3-}$,¹³ but this can simply be the result of the bulkier bridging iodine atoms. In fact, the $\text{Mo}-(\mu\text{-X})\text{-Mo}$ angles in our compounds (average 65.8° for **1** and 65.9° for **3**) are very similar to those found in the above mentioned anions (64.5° in $\text{Mo}_2\text{Cl}_9^{3-}$ and 64.88° in $\text{Mo}_2\text{Br}_9^{3-}$)¹³ and are indicative of a bonding interaction between the metal atoms.^{5b} Such an interaction is also suggested by the NMR results (vide infra).

The Mo–I distances are all in the narrow range 2.75–2.82 Å, and the ones involving bridging iodides are *not* significantly longer than those involving terminal ones, with the exception of those trans to the phosphine groups, presumably because of a trans influence of the latter.

(c) **NMR Studies.** Compound **2** has not been structurally characterized, but its formulation as the NMe_4^+ salt of $[\text{Mo}_2\text{I}_7(\text{PMe}_3)_2]^-$ is proved by the analytical data and by ^1H NMR. The latter shows the resonances of the interstitial THF molecules, of the NMe_4^+ cation, and of the PMe_3 ligands. The resonances of the PMe_3 ligands appear as two singlets at -2.43 and -3.12 in acetone- d_6 at room temperature and closely correspond to those found for **3** in CD_2Cl_2 (δ -2.18 and -2.84). Four features are unusual in these patterns: (i) One and not two resonances are expected for the structure found in the solid state for compounds **1** and **3**, possibly split into a doublet by $^1\text{H}\text{-}^{31}\text{P}$ coupling. (ii) The two peaks are too far from each other to be the result of a H–P coupling (132–138 Hz), and at any rate, they do not have a 1:1 relative intensity. We therefore conclude that we do not observe the expected $^1\text{H}\text{-}^{31}\text{P}$ coupling. (iii) The relative intensities of the two peaks are different when spectra are taken at different times. (iv) Finally, the peaks appear at fields much higher than those typical of coordinated PMe_3 molecules (e.g. δ $+1.76$ for $\text{Mo}_2\text{I}_4(\text{PMe}_3)_4$ in C_6D_6).¹

We observed that the relative intensity of the two PMe_3 peaks becomes practically 1:2 when spectra are taken a long time after dissolution. This leads us to suggest that a *syn*–*gauche* interconversion is taking place in solution and that the energy difference between the two configurations is negligible compared to kT , leading to the statistical 1:2 distribution at equilibrium. The signal of relative intensity 1 (at lower fields) is therefore assigned to the *syn* isomer, while that of relative intensity 2 (at higher fields) is assigned to the *gauche* isomer. Figure 4 shows spectra taken at different times after dissolution of the solid sample (which is pure *syn*) in acetone- d_6 . A plot of $\ln [x_{\text{eq}}/(x_{\text{eq}} - x)]$ against time (x being the concentration of the *gauche* isomer and the equilibrium *syn*:*gauche* distribution being assumed to be 1:2) shows the ex-

pected linearity up to about 2 half-lives, with a slope $(k_1 + k_{-1}) = (1.15 \pm 0.02) \times 10^{-3} \text{ s}^{-1}$.



Again assuming a 1:2 equilibrium distribution, i.e. $K = k_1/k_{-1} = 2$, we obtain $k_1 = (7.67 \pm 0.14) \times 10^{-4} \text{ s}^{-1}$ and $k_{-1} = (3.83 \pm 0.07) \times 10^{-4} \text{ s}^{-1}$, corresponding to activation free energies of 21.4 and 21.8 kcal/mol for ΔG^\ddagger_1 and ΔG^\ddagger_{-1} , respectively, at 20°C . A possible mechanism of isomerization involves conversion of a bridging iodide to a terminal position and rearrangement of the coordination sphere of the resulting five-coordinate molybdenum atom. We do not suggest predissociation of a phosphine or a terminal iodide, since these ligands are substitutionally very inert in molybdenum(III) systems, although we have no proof of this, such as might be obtained from kinetic studies of the *syn*–*gauche* isomerism performed in the presence of excess ligands or with the determination of the independent activation parameters.

The high-field chemical shifts of the PMe_3 ^1H NMR resonances are in agreement with weak paramagnetism. The magnetic behavior of face-sharing bioctahedral Mo(III) dimers has been studied in detail on chloride and bromide systems with variable-temperature magnetic susceptibility techniques. $\text{Cs}_3\text{Mo}_2\text{Cl}_9$ has only a temperature-independent paramagnetism (TIP), while $\text{Cs}_3\text{Mo}_2\text{Br}_9$ possesses a weak, temperature-dependent paramagnetism, indicative of a spin-singlet ground state with a slight temperature-dependent population of one or more paramagnetic excited states.¹⁴ This difference has been attributed to a weaker interaction between the transition-metal atoms with bridging bromide ions, and this is supported by the longer Mo–Mo distance for the bromide complex.¹⁴ Our $[\text{Mo}_2\text{I}_7(\text{PMe}_3)_2]^-$ ion exhibits an even longer metal–metal distance, and we would therefore expect to see higher magnetic moments and perhaps a more pronounced temperature dependence for the magnetic susceptibilities of compounds **1**–**3**. In fact, a χ value of 846×10^{-6} cgsu at 298 K per mole of compound **2** (1409×10^{-6} cgsu after diamagnetic correction for the ligands and the interstitial THF molecules) was measured. This corresponds to an effective magnetic moment of $1.83 \mu_{\text{B}}$ /dimer (or $1.29 \mu_{\text{B}}$ /Mo atom), to be compared with $\chi_{\text{A}} = 250 \times 10^{-6}$ cgsu at 300 K for $\text{Cs}_3\text{Mo}_2\text{Br}_9$ ($\mu_{\text{eff}} = 0.8 \mu_{\text{B}}$ /atom) and with $\chi_{\text{A}} = 160 \times 10^{-6}$ cgsu, independent of temperature, for $\text{Cs}_3\text{Mo}_2\text{Cl}_9$ ($\mu_{\text{eff}} = 0.6 \mu_{\text{B}}$ /atom at room temperature).¹⁴ This behavior is intermediate between those of isoelectronic chromium complexes (with magnetically dilute metal

(13) Saillant, R.; Jackson, R. B.; Streib, W. E.; Foltling, K.; Wentworth, R. A. D. *Inorg. Chem.* **1971**, *10*, 1453.

(14) Saillant, R.; Wentworth, R. A. D. *Inorg. Chem.* **1969**, *8*, 1226.

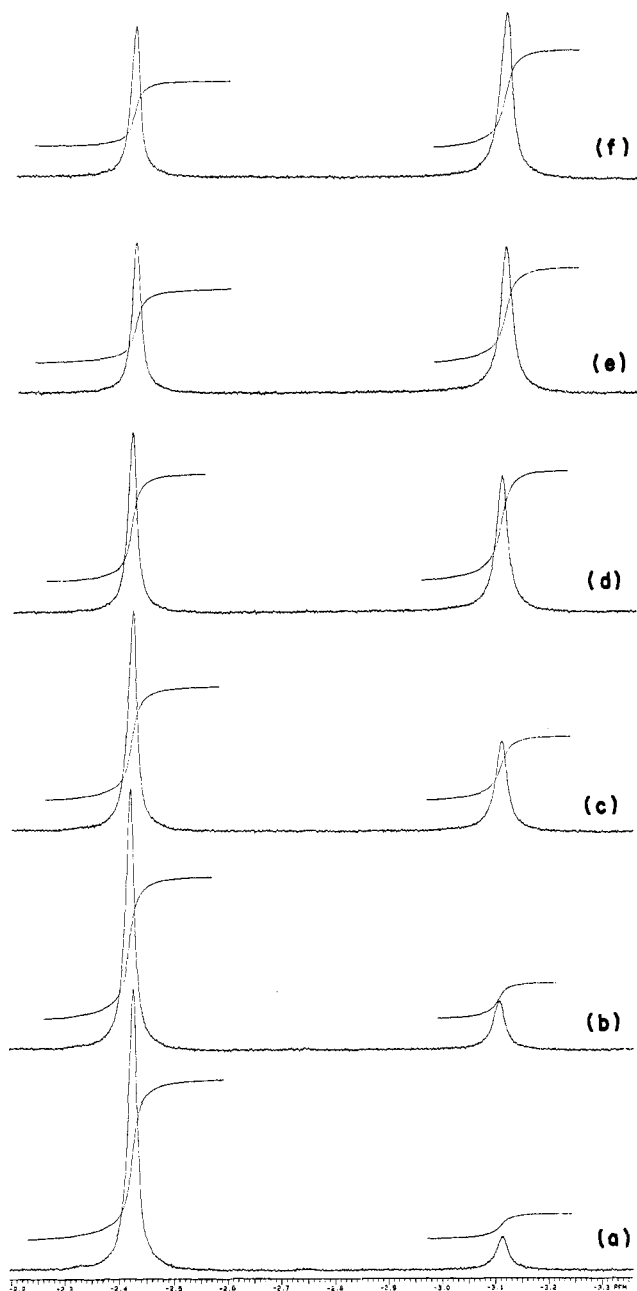


Figure 4. PMe_3 resonances in the ^1H NMR spectrum of compound **2** (CD_3COCD_3 , 20°C) at the following times after dissolution: (a) 3 min; (b) 5 min; (c) 10 min; (d) 20 min; (e) 30 min; (f) 40 min.

atoms) and tungsten complexes (with stronger metal-metal interactions and only a temperature-independent paramagnetism).¹⁵

We are not equipped to carry out a variable-temperature magnetic susceptibility study, but we observed a substantial

(15) Saillant, R.; Wentworth, R. A. D. *Inorg. Chem.* **1968**, *7*, 1606.

temperature dependence of the PMe_3 ^1H NMR chemical shifts for compound **3**. The direction of the shifts agrees with a higher paramagnetism at higher temperatures. This can, of course, be the result of two separate effects: the intrinsic temperature dependence of the magnetic susceptibility for the paramagnetic excited state(s), and the temperature effect on the Boltzmann distribution over the energy levels. A treatment of the chemical shift temperature dependence for simpler antiferromagnetically coupled dinuclear systems is available.¹⁶

The δ values for both isomers of compound **3** are linearly dependent on T^{-1} over the entire temperature range studied (193–293 K). We cannot, however, draw quantitative conclusions from these data since our temperature range is, for technical reasons, rather limited, and we do not have a thorough knowledge of the paramagnetic excited state(s). We can only point out that, as shown by the different slopes in a δ vs T^{-1} plot, the two isomers exhibit a small but significant difference between their spin exchange interactions.

The compound $[\text{PPh}_4][\text{Mo}_2\text{Cl}_7(\text{SMe}_2)_2]$, whose structure is identical with those of the compounds described in this paper, is also said¹⁷ to possess temperature-dependent ^1H NMR properties in agreement with antiferromagnetic coupling of the molybdenum ions.

We can now explain the failure to observe any ^1H - ^{31}P coupling in the ^1H NMR spectrum of compounds **2** and **3** as being due to ^{31}P nuclear spin relaxation caused by its proximity to the paramagnetic center. We were unable to observe any ^{31}P NMR signal, even at -80°C , nor were the carbon signals of PMe_3 observed in the room-temperature ^{13}C NMR spectrum.

Conclusions

$[\text{Mo}_2\text{I}_7(\text{PMe}_3)_2]^-$ is the first iodide-bridged face-sharing biocuboidal Mo(III) dimer reported in the literature. The structural parameters, the magnetic susceptibility, and the NMR studies all indicate that its behavior is analogous to that of its chloride- and bromide-bridged analogues and intermediate between those of the corresponding chromium and tungsten species. However, the longer metal-metal distance caused by the bulkier halide makes this ion magnetically more active.

Acknowledgment. We are grateful to the National Science Foundation for support of this work. We would also like to thank Prof. J. F. Haw and S. Kitagawa for helpful discussions.

Supplementary Material Available: Full tables of bond distances and angles and anisotropic displacement parameters for compounds **1** and **3** and figures showing a plot of $\ln [x_{\text{eq}}/(x_{\text{eq}} - x)]$ vs time (from the data of Figure 4) and a plot of the PMe_3 ^1H NMR chemical shifts vs T^{-1} for the syn and gauche isomers of compound **3** (8 pages); listings of observed and calculated structure factors for **1** and **3** (23 pages). Ordering information is given on any current masthead page.

- (16) (a) La Mar, G. N.; Eaton, G. R.; Holm, R. H.; Walker, F. A. *J. Am. Chem. Soc.* **1973**, *95*, 63. (b) Bertini, I.; Luchinat, C. *NMR of Paramagnetic Molecules in Biological Systems*; Benjamin/Cummings: Menlo Park, CA, 1986.
- (17) Boorman, P. M.; Moynihan, K. J.; Oakley, R. T. *J. Chem. Soc., Chem. Commun.* **1982**, 899.